Organic Electronics 15 (2014) 1413–1421

Contents lists available at ScienceDirect

Organic Electronics

journal homepage: www.elsevier.com/locate/orgel

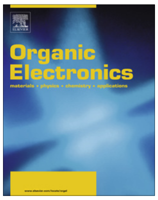

Synthesis of phenylcarbazole–thiophene-based structural isomers as unipolar host materials for blue PHOLEDs and their device performance

Seung-Won Choi, Jun Yeob Lee, Seok-Ho Hwang [*]

Department of Polymer Science & Engineering, Dankook University, Yongin, Gyeonggi 448-701, Republic of Korea

A R T I C L E I N F O

Article history:
Received 12 January 2014
Received in revised form 25 March 2014
Accepted 4 April 2014
Available online 18 April 2014

Keywords:
Phenylcarbazole
Thiophene
Phosphorescent OLEDs
Host material
Symmetry

A B S T R A C T

New high triplet-energy host materials, which are symmetrically or asymmetrically designed by using phenylcarbazole and thiophene moieties, were synthesized by Suzuki–Miyaura cross-coupling reactions and their device performances of blue phosphorescent organic light-emitting diodes were also investigated. The synthesized compounds showed a high triplet energy (>2.84 eV) and good thermal stability. Highly efficient blue PHOLEDs were obtained when employing the symmetric compounds having C2 symmetry as the host material and *bis*[2-(4,6-difluorophenyl)pyridinato-C^2,*N*](picolinato)iridium(III) (FIrpic) as the guest material. Their maximum external quantum efficiency of the device reached as high as 18.9% with blue color coordinate of (0.15, 0.35).

1. Introduction

For more than ten years, much progress has been made in the field of phosphorescent organic light-emitting diodes (PHOLEDs) because they effectively harvest electro-generated singlet and triplet excitons to accomplish internal quantum efficiency close to 100%, which is much superior to the 25% upper limit imposed by the formation of singlet excitons in fluorescence [1–4]. To realize highly efficient PHOLEDs, a suitable host material is usually employed to suppress the intrinsic detrimental effects, such as aggregation quenching and/or triplet–triplet annihilation, of transition metal-centered phosphors [5,6]. However, designing host materials having higher triplet energy levels than that of the phosphorescent dopant still remains a challenge for materials researchers.

As part of an ongoing effort, many researches have been conducted to establish structure–property relationships for developing new host materials with desired properties in an intelligent way. Those systematic studies on conjugated compounds also provide valuable insights into relevant fundamental properties of PHOLEDs [7–10]. The selection of building blocks has to be carefully examined in the molecular design of functional materials because they tend to dominate the properties in many cases. Among many heteroaromatic systems, carbazoles and their derivatives are a highly interesting family of functional organic molecules because carbazole has fine optical properties, a low redox potential, and high chemical stability. Thus, carbazole would be recognized as a useful scaffold to allow the large structural diversity for fine tuning of optical and electrochemical properties.

Thiophene derivatives are now excellent candidates for a variety of advanced materials applications [11,12]. Therefore, mixed π-conjugated polymers and oligomers made of carbazoles and thiophenes are a new class of functional compounds through the use of their highly electrondonating ability. Some compounds consisting of carbazole and thiophene moieties were also synthesized

---

[*] Corresponding author. Tel.: +82 31 8005 3588; fax: +82 318021 7218.
E-mail address: bach@dankook.ac.kr (S.-H. Hwang).

http://dx.doi.org/10.1016/j.orgel.2014.04.006
1566-1199/© 2014 Elsevier B.V. All rights reserved.

[13–21]; however, no systematic study on structurally well-defined carbazole–thiophene systems focusing on the effect of the conjugation connectivity between the carbazole and thiophene moieties on their electronical, photophysical, and electroluminescent properties has been reported so far, to the best of our knowledge.

In this context, we became interested in phenylcarbazole-substituted thiophene derivatives, in which two phenylcarbazole moieties are symmetrically or asymmetrically incorporated into a thiophene moiety at the 3-, and 4-positions (Scheme 1). A series of host materials varying the isomeric chemical structures allow us to study the structure–property relationships of phenylcarbazole–thiophene-based host materials. Here, we report the synthesis of symmetrical and asymmetrical isomeric materials and their device performances.

2. Experimental

2.1. General procedure

Chemicals were commercially purchased and used without further purification. Thin layer chromatography (TLC) was conducted on flexible sheets (Baker-flex) precoated SiO_2 (IB2-F) and visualized by UV light. Column chromatography was conducted using SiO_2 (60–200 mesh) from Fisher Scientific. Melting points were determined on MEL-TEMP, model 1102D. ^{1}H and ^{13}C NMR spectra were recorded on Jeol ECS-400 NMR spectrometer using $CDCl_3$, as the solvent, except where noted. Mass spectra obtained on Agilent Technology 6100 Series Electrospray Ion Trap mass spectrometer (ESI-MS). Photophysical properties of the synthesized compounds were analyzed using ultraviolet–visible (UV–Vis) and photoluminescence (PL) spectrometer. The synthetic compounds were dissolved in tetrahydrofuran at a concentration of 1.0×10^{-4} M for UV–Vis and PL measurements. Triplet energy analysis of the synthesized compounds was carried out using low temperature PL measurement in liquid nitrogen (77 K). Energy levels of the synthesized compounds were measured using cyclic voltammetry (CV). Cyclic voltammetry measurement of organic materials was carried out in acetonitrile solution with tetrabutylammonium perchlorate at 0.1 M concentration. Ag was used as the reference electrode and Pt was the counter electrode. Organic materials were coated on indium–tin–oxide substrate and were immersed in electrolyte for analysis. Ferrocene was used as the internal standard material. High performance liquid chromatography (HPLC) analysis of the synthesized materials was carried out using HPLC from Younglin Instrument. Glass transition temperature of the materials was measured using a differential scanning calorimeter (DSC; Mettler-Toledo DSC 820) at a heating rate of 10 °C min^{-1} under nitrogen atmosphere. Thermogravimetric analysis (TGA) was conducted with a Mettler-Toledo TG50 at a heating rate of 20 °C min^{-1} under a nitrogen atmosphere.

2.2. Synthesis

2.2.1. 9-(4-Bromophenyl)-9H-carbazole (1)

A solution of 1,4-dibromobenezne (14.2 g, 60.0 mmol), carbazole (5 g, 30.0 mmol), CuI (0.3 g, 1.5 mmol), 18-crown-6 (0.4 g, 1.5 mmol), K_2CO_3 (6.24 g, 45.0 mmol) in DMF (10 ml) was refluxed for overnight under N_2. The reaction mixture was cooled down to room temperature, poured into H_2O and then extracted with dichloromethane. The combined organic layer was washed with brine and dried over magnesium sulfate. The solvent was removed *in vacuo* and crude product was purified by chromatography (SiO_2) eluting with an *n*-hexane to give a white solid (5.05 g, 57%): m.p. = 131 °C; ^{1}H NMR δ 8.13 (d, 2H), 7.72 (d, 2H), 7.45 (d, 2H), 7.38 (m, 4H), 7.29 (t, 2H); ^{13}C NMR

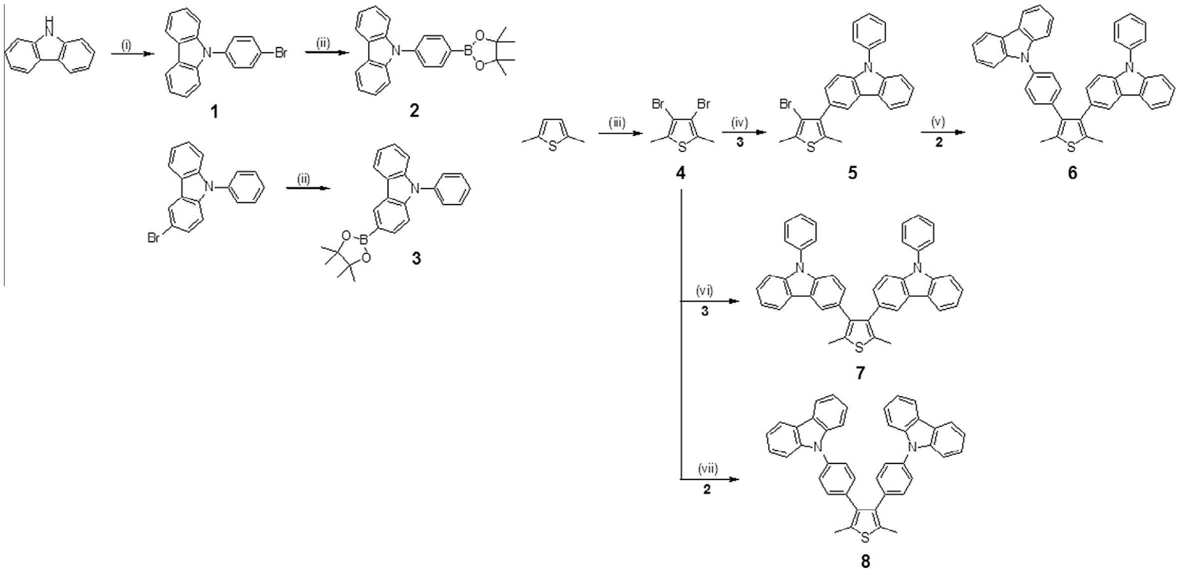

Scheme 1. *Reagents and conditions*: (i) 1,4-dibromobenzene, CuI, K_2CO_3, 18-crown-6, DMF, reflux; (ii) *bis*(pinacolate)diboron, KOAc, $PdCl_2$(dppf), 1,4-dioxane, reflux; (iii) Br_2, AcOH, 0 °C; (iv–vii) 2 M K_2CO_3, $Pd(PPh_3)_4$, 110 °C, 24–36 h.

δ 140.7, 136.9, 133.2, 128.8, 126.2, 123.6, 121.0, 120.5, 120.3, 109.7.

2.2.2. General Miyaura borylation procedure

A solution of haloarene (1.0 mmol ratio), *bis*(pinacolate)diboron (1.2 mmol ratio), KOAc (1.5 mmol ratio), and $PdCl_2$(dppf) (0.02 mmol ratio) in dry 1,4-dioxane (20 ml) was refluxed for overnight under N_2. After being cooled to room temperature, the mixture was poured into H_2O and then extracted with dichloromethane. The combined organic layer was washed with brine and dried over magnesium sulfate. The solvent was removed *in vacuo* and crude product was purified by chromatography (SiO_2) eluting with a mixture of DCM and *n*-hexane to afford the pure products.

2.2.3. 9-(4-(4,4,5,5,-Tetramethyl-1,3,2-dioxaborolan-2-yl)phenyl)-9H-carbazole (2)

9-(4-Bromophenyl)-9*H*-carbazole (5.5 g, 17.19 mmol), *bis*(pinacolate)diboron (5.24 g, 20.63 mmol), KOAc (2.63 g, 25.76 mmol), and $PdCl_2$(dppf) (0.15 g, 0.02 mmol) were used to yield compound **2** (5.36 g, 85.1%) as a white solid: m.p. = 170 °C; ^{1}H NMR δ 8.08 (d, 1H), 8.02 (d, 1H), 7.63 (d, 1H), 7.41 (m 5H), 7.29 (m, 4H), 1.23 (s, 12H); ^{13}C NMR δ 140.7, 140.5, 136.5, 126.2, 123.6, 120.4, 120.2, 110.0, 84.2, 25.1.

2.2.4. 9-Phenyl-3-(4,4,5,5,-tetramethyl-1,3,2-dioxaborolan-2-yl)-9H-carbazole (3)

3-Bromo-9-phenyl-9*H*-carbazole (4 g, 12.4 mmol), *bis*(pinacolate)diboron (3.79 g, 14.9 mmol), KOAc (1.9 g, 18.6 mmol), and $PdCl_2$(dppf) (0.14 g, 0.02 mmol) were used to yield compound **3** (4.1 g, 88.4%) as a white solid: m.p. = 160 °C; ^{1}H NMR δ 8.63 (s, 1H), 8.10 (d, 1H), 7.95 (d, 1H), 7.58 (m, 5H), 7.41 (m, 4H), 1.23 (s, 12H); ^{13}C NMR δ 143.1, 141.1, 137.6, 132.5, 130.0, 127.8, 127.7, 126.1, 123.6, 123.2, 120.6, 120.4, 109.9, 109.2, 83.8, 25.1.

2.2.5. 3,4-Dibromo-2,5-dimethylthiophene (4)

A solution of 2,5-dimethylthiophene (5 g, 44.7 mmol) in glacial acetic acid (50 ml) was added dropwise to a bromine (10.7 g, 133.7 mmol) at 0 °C. The mixture was stirred for overnight at room temperature. The reaction mixture was poured into H_2O and then extracted with diethyl ether. The combined organic layer was washed with brine and dried over magnesium sulfate. The solvent was removed *in vacuo* and crude product was purified by chromatography (SiO_2) eluting with an *n*-hexane to give a white solid (8 g, 67%): m.p. = 46 °C; ^{1}H NMR δ 2.54 (s, 6H); ^{13}C NMR δ 132.7, 109.5, 14.1.

2.2.6. General Suzuki–Miyaura cross-coupling procedure

A mixture of **4** (1 equiv.), boronic acid pinacol ester (1.2–2.4 equiv.) and 2 M K_2CO_3 (10 ml) in toluene was bubbled with argon with stirring for 30 min. $Pd(PPh_3)_4$ (0.02–0.04 equiv.) was added to the mixture, and the resulting mixture was refluxed for overnight under argon atmosphere. The reaction mixture was cooled down to room temperature, poured into H_2O and then extracted with dichloromethane. The combined organic layer was washed with brine and dried over magnesium sulfate. The solvent was removed *in vacuo* and the residue was purified by SiO_2 column chromatography. The final pure materials were obtained by sublimation.

2.2.7. 3-(4-Bromo-2,5-dimethylthiophene-3-yl)-9-phenyl-9H-carbazole (5)

3 (1.62 g, 4.40 mmol), **4** (1 g, 3.70 mmol), 2 M K_2CO_3 solution (10 ml), and $Pd(PPh_3)_4$ (0.05 g, 0.04 mmol) were used for general Suzuki–Miyaura cross-coupling reaction. The crude product was purified by chromatography (SiO_2) eluting with a mixture of DCM: *n*-hexane (1:2; v/v) to give a white solid (0.96 g, 60%): m.p. = 155 °C; ^{1}H NMR δ 8.13 (d, 1H), 8.04 (s, 1H), 7.62 (m, 3H), 7.44 (m, 3H), 7.29 (m, 2H), 2.42 (d, 6H); ^{13}C NMR δ 141.9, 141.5, 141.3, 137.5, 130.5, 128.2, 127.2, 126.9, 126.7, 124.0, 123.7, 123.1, 121.5, 120.7, 118.3, 110.6, 110.2, 109.6, 15.4, 11.9.

2.2.8. 9-(4-(2,5-Dimethyl-4-(9-phenyl-9H-carbazol-6-yl)thiophen-3-yl)phenyl)-9H-carbazole (6)

A solution of **5** (0.96 g, 2.22 mmol), **2** (0.98 g, 2.66 mmol) 2 M K_2CO_3 solution (10 ml), and $Pd(PPh_3)_4$ (0.1 g, 0.09 mmol) were used for general Suzuki–Miyaura cross-coupling reaction. The crude product was purified by chromatography (SiO_2) eluting with a mixture of DCM: *n*-hexane (2:3; v/v) to give a white solid (0.73 g, 55%): m.p. = 242 °C; ^{1}H NMR δ 8.13 (s, 1H), 8.11 (d, 1H), 8.09 (d, 1H), 7.89 (s, 1H), 7.62 (m, 3H), 7.54 (m, 4H), 7.45 (m, 4H), 7.33 (m, 4H), 7.29 (m, 4H), 7.13 (d, 1H), 2.56 (d, 6H); ^{13}C NMR δ 141.4, 141.0, 139.8, 138.6, 137.9, 136.8, 135.7, 131.8, 131.5, 131.3, 129.8, 128.5, 128.2, 127.4, 127.1, 126.9, 126.7, 126.1, 126.0, 125.9, 123.4, 123.3, 122.2, 120.0, 119.5, 110.0, 109.8, 109.2, 14.1; ESI-MS: *m/z* 594.2 $[M]^+$ (calcd. *m/z* 594.2).

2.2.9. 3-(2,5-Dimethyl-4-(9-phenyl-9H-carbazol-6-yl)thiophen-3-yl)-9-phenyl-9H-carbazole (7)

A solution of **3** (3.28 g, 8.89 mmol), **4** (1 g, 3.70 mmol), 2 M K_2CO_3 solution (20 ml), and $Pd(PPh_3)_4$ (0.1 g, 0.09 mmol) were used for general Suzuki–Miyaura cross-coupling reaction. The crude product was purified by chromatography (SiO_2) eluting with a mixture of DCM: *n*-hexane (1:1; v/v) to give a white solid (1.19 g, 54%): m.p. = 237.0 °C; ^{1}H NMR δ 8.03 (d, 2H), 7.96 (s, 2H), 7.55 (q, 6H), 7.39 (m, 6H), 7.22 (m, 6H), 7.07 (d, 2H), 2.49 (s, 6H); ^{13}C NMR δ 141.2, 140.6, 139.8, 137.7, 131.0, 130.0, 129.7, 128.5, 127.7, 127.2, 125.6, 123.9, 123.2, 122.2, 120.4, 120.0, 110.2, 109.6, 14.2; ESI-MS: *m/z* 594.2 $[M]^+$ (calcd. *m/z* 594.2).

2.2.10. 9-(4-(4-(4-(9H-carbazol-9-yl)phenyl)-2,5-dimethylthiophen-3-yl)phenyl)-9H-carbazole (8)

A solution of **2** (3.28 g, 8.89 mmol), **4** (1 g, 3.70 mmol), 2 M K_2CO_3 solution (20 ml), and $Pd(PPh_3)_4$ (0.1 g, 0.09 mmol) were used for general Suzuki–Miyaura cross-coupling reaction. The crude product was purified by chromatography (SiO_2) eluting with a mixture of DCM: *n*-hexane (1:1; v/v) to give white solid (1.23 g, 56%): m.p. = 303 °C; ^{1}H NMR δ 8.16 (d, 2H), 7.51 (d, 2H), 7.40 (m, 20H), 2.49 (s, 6H); ^{13}C NMR δ 141.1, 138.5, 136.2, 132.5, 131.7, 126.8, 126.2, 120.4, 120.1, 109.8, 14.1; ESI-MS: m/z 594.2 $[M]^+$ (calcd. m/z 594.2).

2.3. Fabrication of PHOLED device and measurements

The device structure of blue PHOLEDs was indium tin oxide (ITO, 150 nm)/*N*,*N*′-diphenyl-*N*,*N*′-bis-[4-(phenyl-*m*-tolyl-amino)-phenyl]-biphenyl-4,4′-diamine (DNTPD, 60 nm)/*N*,*N*′-di(1-naphthyl)-*N*,*N*′-diphenylbenzidine (NPB, 15 nm)/4,4′-cyclohexylidenebis[*N*,*N*-bis(4-methylphenyl) benzenamine] (TAPC, 10 nm)/*N*,*N*′-dicarbazolyl-3,5-benzene (mCP, 10 nm)/host: bis[2-(4,6-difluorophenyl)pyridinato-C^2,*N*](picolinato)iridium(III) (FIrpic) (25 nm, 10%)/4-(triphenylsilyl) phenyldiphenylphosphine oxide (TSPO1, 35 nm)/LiF (1 nm)/Al (200 nm). The doping concentration of FIrpic was 10%. The device performances of the blue PHOLEDs were measured with Keithley 2400 source measurement unit and CS1000 spectroradiometer.

3. Results and discussion

In our molecular design, two phenylcarbazole moieties were incorporated into a thiophene symmetrically and asymmetrically (Scheme 1). Compound **1** was synthesized via Ullmann coupling reaction [22] in the presence of copper iodide and K_2CO_3. To combine between phenylcarbazole and thiophene, boronic ester were first introduced to the 3-bromo-9-phenylcarbazole and 9-(4-bromophenyl)-9*H*-carbazole by Miyaura borylation reaction [23] with *bis*(pinacolate)diboron.

Synthesis of asymmetric host material, **6**, began with commercially available 2,5-dimethylthiophene, which was brominated with bromine to give **4** (67%) that was subsequently conducted selective Suzuki–Miyaura cross-coupling reaction [24] in the presence of $Pd(PPh_3)_4$ as a catalyst with **3** to form the intermediate, **5** (60%). And then, same cross-coupling reaction was performed on **5** with **2** to give desired asymmetric host material, **6**. The Suzuki–Miyaura cross-coupling reaction of **4** with **2** and **3** gave to symmetric host materials, **7** and **8**, respectively. All compounds were fully characterized by various spectroscopic methods, such as ^{1}H, ^{13}C NMR, and mass spectroscopy.

The thermal behavior under heating of the compounds was studied by TGA and DSC under a nitrogen atmosphere (Table 1). The glass transition temperatures of **6**–**8** were clearly appeared to be 125, 110, and 133 °C, respectively. The glass transition temperature of **6** with different moieties in the molecular structure was in between that of **7** and **8** with the same moieties in the backbone structure. Their glass transition temperatures are higher than that of the mCP (55 °C) [25] due to more bulky and dense chemical structures. Also, the decomposition temperatures at initial 5 wt.% loss for **6**–**8** were 376, 366, and 390 °C, respectively. These results mean that they might be suitable to use as PHOLED component because the high thermal stability could improve the lifetime of the devices [26–28].

Thermal stability of the host materials was further studied by monitoring morphological change of the vacuum deposited host films. Fig. 1 shows optical microscopic pictures of the host materials after thermal annealing at various temperatures. Crystallization of **7** and **8** was observed after thermal annealing at 120 °C, while no crystallization of **6** appeared up to 130 °C. Although the glass transition temperature of **6** was lower than that of **8**, asymmetric molecular structure of **6** suppressed crystallization of the host material, resulting in stable morphology.

Spatial distributions of the highest occupied molecular orbital (HOMO) and the lowest unoccupied molecular orbital (LUMO) of **6**–**8** were calculated with the Gaussian program at the B3LYP/6-31G(d) level, using the density function theory (DFT) for the geometry optimizations. As shown in Fig. 2, the HOMO of **6** and **8** is mainly localized at the phenylcarbazole moiety linked with thiophene unit, whereas those LUMO showed a different behavior. The LUMO of **6** was mainly localized to another phenylcarbazole moiety; however, in the case of **8**, the LUMO was populated over the two phenyl unit and thiophene unit. The HOMO of **7** is situated over whole molecules but the LUMO is localized at two phenylcarbazole backbone with limited contribution for the thiophene unit.

The photophysical properties of the synthesized compounds were analyzed by using UV/Vis and PL measurements (Table 1). Solution UV–Vis absorption, solution PL and low temperature PL emission spectra of **6**–**8** are shown in Fig. 3. Weak UV–Vis absorption peaks assigned to n–π^* transition of the thiophene and carbazole moieties were observed between 310 nm and 360 nm, and strong absorption peaks corresponding to π–π^* absorption of the carbazole linked thiophene backbone appeared below 300 nm. The absorption edges of the UV/Vis spectra for **6**–**8** were 358, 362, and 351 nm, which corresponded to the bandgap at 3.46, 3.42, and 3.53 eV, respectively. The triplet energies of **6**–**8** were 2.84, 2.85, and 3.00 eV, which could be calculated from the first phosphorescent emission peak of low temperature (77 K) PL spectrum at 436, 434, and 413 nm, respectively. The bandgap and triplet energy of **6** and **7** were lower than those of **8** due to extension of conjugation though 3-position of carbazole unit. Their triplet energies were enough to use the host material as a blue phosphorescent dopant. The triplet energy of the *bis*

Table 1
Material characteristics of **6**–**8**.

Compound	λ_{abs} (nm)	λ_{em} (nm)	E_g (eV)	E_T (eV)	HOMO (eV)	LUMO (eV)	T_g (°C)	T_m (°C)	T_d (°C)
6	358	436	3.46	2.84	−6.03	−2.57	125	254	376
7	363	434	3.42	2.85	−5.90	−2.48	110	230	366
8	351	413	3.53	3.00	−6.06	−2.53	133	301	390

Abbreviations: λ_{abs}, absorption edge; λ_{em}, emission maximum; E_g, energy gap calculated from the onset absorption wavelength; E_T, triplet energy calculated from the highest-energy fluorescence peak; T_g, glass transition temperature; T_m, melting temperature; T_d, decomposition temperature at 5 wt.% weight loss.

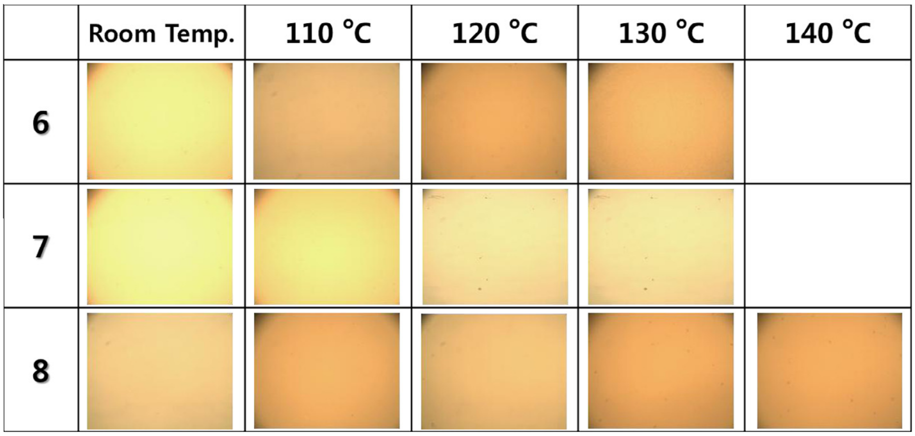

Fig. 1. Optical microscope images of **6**–**8** after thermally annealing around T_g.

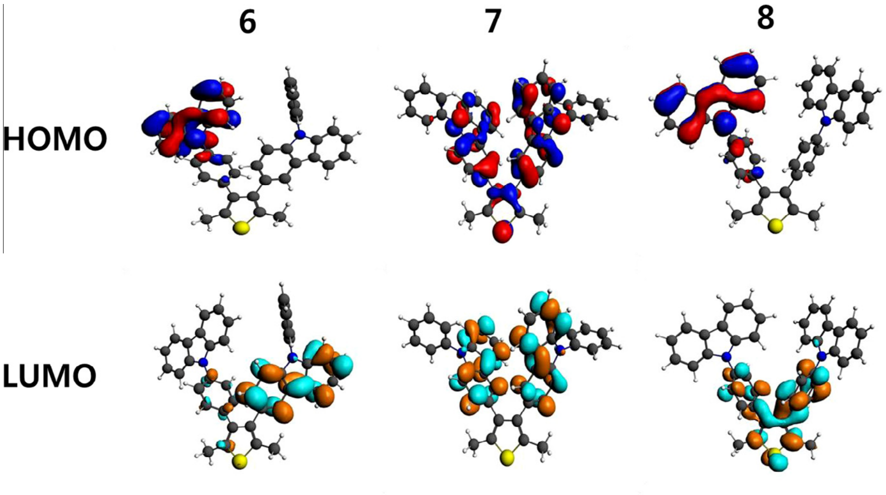

Fig. 2. HOMO and LUMO distributions of **6**–**8**.

[2-(4,6-difluorophenyl)pyridinato-C^2,N](picolinato)iridium(III) (FIrpic) dopant is 2.70 eV and effective energy transfer from synthesized hosts to FIrpic dopant is expected.

On the basis of the electrochemical oxidation onset potential, the HOMO energy levels of **6**–**8** were estimated as −6.03, −5.90, and −6.06 eV, respectively. The LUMO energy levels of **6**–**8** were −2.57, −2.48, and −2.53 eV, calculated from the HOMO energy level and energy bandgap determined from the UV/Vis absorption threshold.

Hole- and electron-only devices composed of **6**–**8** were fabricated to compare the hole and electron density in the host materials. Fig. 4 shows the current density–voltage curves of hole- and electron-only devices bearing **6**–**8**. All host materials showed higher hole current density than electron current density because of hole transport type carbazole moieties in the backbone structure. In addition, hole and electron current density of symmetric compounds (**7** and **8**) were higher than that of asymmetric compound (**6**).

Hole and electron mobility of the host materials was calculated from single carrier device data and are shown in Fig. 5. All host materials showed higher hole mobility than electron mobility because of carbazole moieties in the molecular structure. The hole mobility of the host materials was higher than that of commercially available 2,6-bis(3-(carbazol-9-yl)phenyl)pyridine (26DCzPPy) host material [29], but the electron mobility was slightly lower than that of 26DCzPPy. This result indicates that **6**–**8** may serve as hole transport type host materials for blue PHOLED.

As the compounds **6**–**8** showed HOMO/LUMO levels for hole and electron injection, and high triplet energy for energy transfer to blue emitting FIrpic, it was evaluated as the host material for FIrpic based blue PHOLEDs. The blue PHOLEDs were fabricated using the host materials with 10% of FIrpic doping concentration in all devices. Fig. 6 shows current density–voltage–luminance curves of the blue PHOLEDs. Just like the current density–voltage data in the single carrier devices (Fig. 4), the current density of the blue

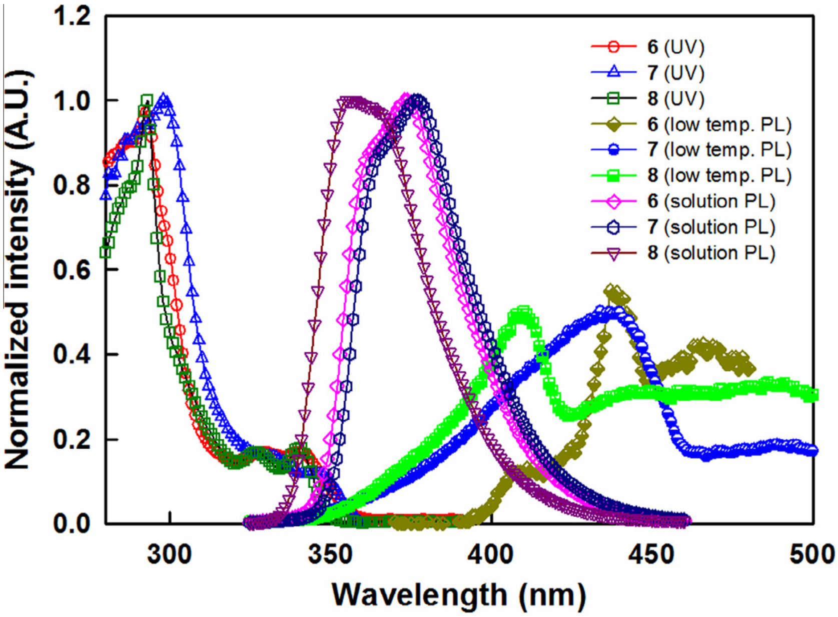

Fig. 3. UV/Vis, solution PL and low temp. PL spectra of **6**–**8**.

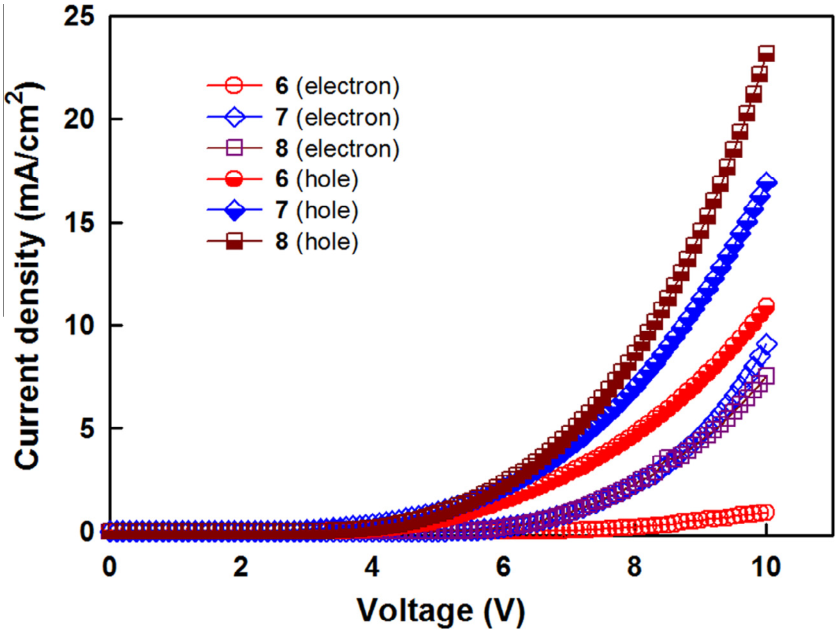

Fig. 4. Current density–voltage curves of hole- and electron-only device made of **6**–**8**.

PHOLED with **7** and **8** having C2 symmetry as the host exhibited higher value compared with that of the blue PHOLEDs with **6** having asymmetry as the host. The magnitude of current density follows the order of **8** > **7** > **6**. This result means that the device performance might be influenced by their structural symmetry between phenylcarbazole and thiophene moieties. The luminance showed the same tendency as the current density.

External quantum efficiency–luminance curves of the blue PHOLEDs with **6**–**8** are presented in Fig. 7. The symmetric compounds (**7** and **8)** device exhibited higher quantum efficiency than the asymmetric compound (**6**) device at the same luminance. The maximum quantum efficiencies of the **7** and **8** devices were 18.9% and 18.5% compared with maximum quantum efficiency of 14.0% of the **6** device. The high quantum efficiencies of the symmetric

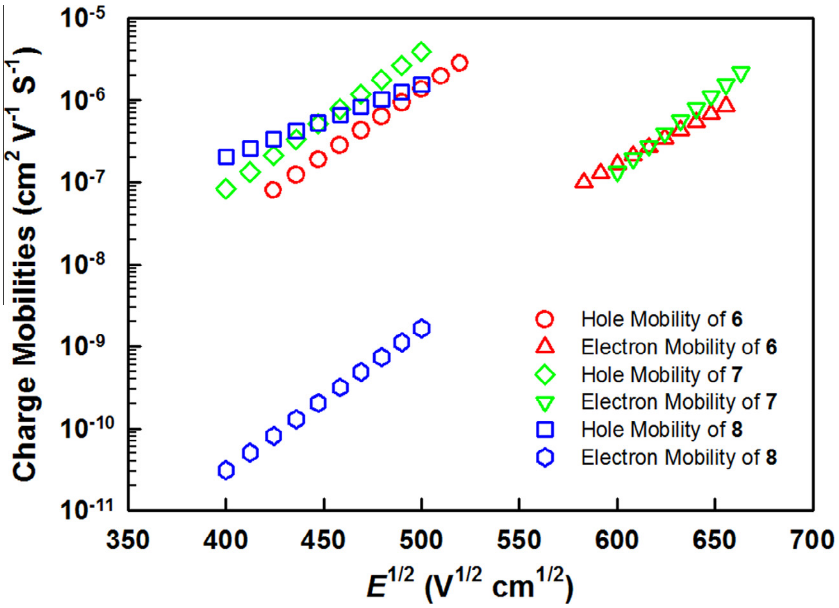

Fig. 5. Charge mobilities of **6**–**8**.

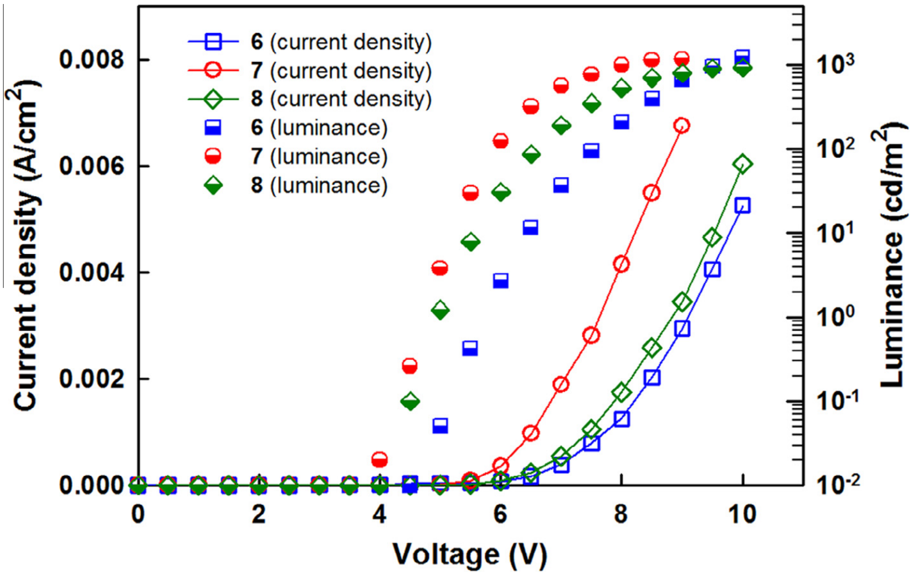

Fig. 6. Current density–voltage–luminance curves of blue PHOLED devices with **6**–**8**. (For interpretation of the references to colour in this figure legend, the reader is referred to the web version of this article.)

compound devices are related with balanced charge density, exciton confinement and efficient energy transfer. Although all host materials showed higher hole current density than electron current density, there was less difference between hole current density and electron current density in the device **7** and **8** than in the device **6**, resulting in high quantum efficiency in device **7** and **8**. In the case of device **6**, the very low electron current density compared to hole current density lead to poor charge balance and low quantum efficiency [30]. Exciton confinement by high triplet energy host, hole transport material and electron transport material also played an important role of enhancing the quantum efficiency of **7** and **8** device. As the triplet energy of the host and charge transport materials was higher than that of FIrpic, triplet excitons of FIrpic could be effectively confined in the emitting layer with little quenching. Finally, efficient energy transfer as can be observed in the electroluminescence (EL) spectra of **7** and **8** device in Fig. 8 was another key factor for the high quantum efficiency of the symmetric compound devices. Only

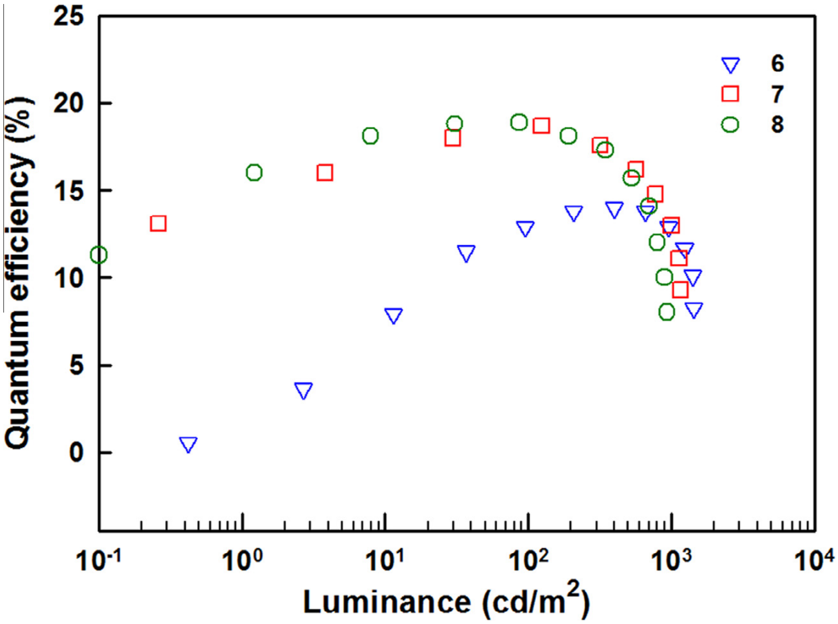

Fig. 7. Quantum efficiency–luminance curves of blue PHOLED devices with **6**–**8**. (For interpretation of the references to colour in this figure legend, the reader is referred to the web version of this article.)

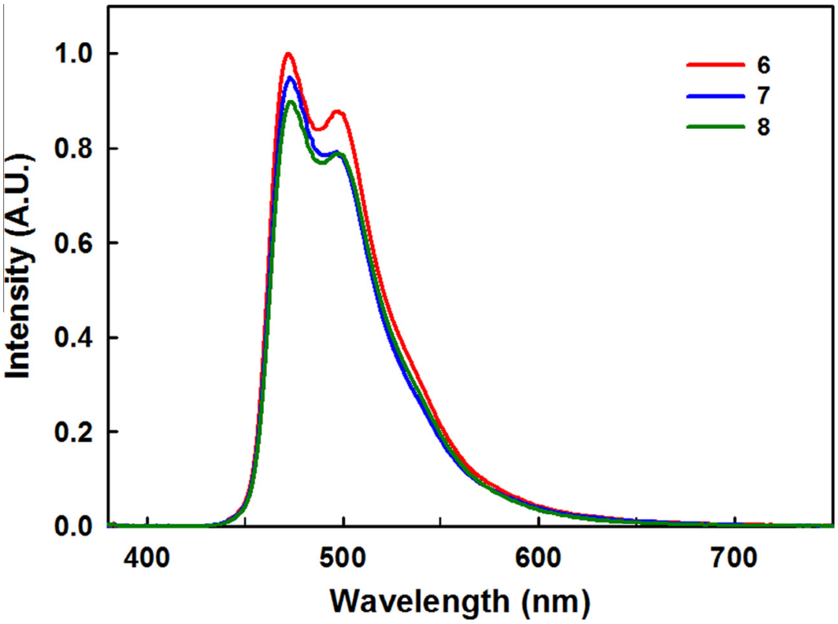

Fig. 8. Electroluminescence spectra of blue PHOLED devices with **6**–**8**. (For interpretation of the references to colour in this figure legend, the reader is referred to the web version of this article.)

blue emission of FIrpic without any emission from **7** and **8** host materials were observed in the EL spectrum, implying good energy transfer from hosts (**7** and **8**) to FIrpic. The low quantum efficiency of the **6** device is due to poor charge balance in the emitting layer because excitons can be effectively confined in the **6** device and no emission from **6** host was observed in the EL spectrum of the **6** device.

EL spectra of the **6**–**8** devices are shown in Fig. 8. Strong blue emission by FIrpic appeared at 472 nm with a shoulder at 497 nm. No other emission peak from host or charge transport materials was observed, confirming effective charge confinement in the emitting layer. Color coordinates of the **6**–**8** devices were (0.16, 0.36), (0.15, 0.35), and (0.16, 0.37), respectively.

4. Conclusions

In summary, three structural isomers designed by symmetric and asymmetric aspect were synthesized by Suzuki–Miyaura cross-coupling reaction. Those compounds showed a high triplet energy (>2.84 eV) and broad bandgap (>3.40 eV) that are suitable to be applied in blue PHOLED as host material. A high maximum quantum efficiency of 18.9% and 18.5% was achieved in the blue PHOLEDs with the symmetric compounds (**7** and **8**) as host material, which was symmetrically constructed by incorporating two phenylcarbazole onto 3,4-position of a thiophene. Therefore, the phenylcarbazole moiety should be symmetrically introduced in the molecular structure of thiophene moiety to manage the charge transport properties of host materials.

Appendix A. Supplementary material

Supplementary data associated with this article can be found, in the online version, at http://dx.doi.org/10.1016/j.orgel.2014.04.006.

References

[1] J. Kido, M. Kimura, K. Nagai, Science 267 (1999) 1332.
[2] S.R. Forrest, Org. Electron. 4 (2003) 45.
[3] W. D'Andrade, S.R. Forrest, Adv. Mater. 16 (2004) 1585.
[4] Y. Chi, P.-T. Chou, Chem. Soc. Rev. 39 (2010) 638.
[5] M.A. Baldo, C. Adachi, S.R. Forrest, Phys. Rev. B: Condens. Matter 62 (2000) 10967.
[6] S.-J. Su, H. Sasabe, T.I. Takeda, J. Kido, Chem. Mater. 20 (2008) 1691.
[7] K. Müllen, G. Wegner, Electronic Materials: The Oligomer Approach, Wiley-Vch, Weinheim, 1998.
[8] R.E. Martin, F. Diederich, Angew. Chem. Int. Ed. 38 (1999) 1350.
[9] J.L. Segura, N.J. Martín, Mater. Chem. 10 (2000) 2403.
[10] W.-C. Lin, W.-C. Huang, M.-H. Huang, C.-C. Fan, H.-W. Lin, L.-Y. Chen, Y.-W. Liu, J.-S. Lin, T.-C. Chao, M.-R. Tseng, J. Mater. Chem. C 1 (2013) 6835.
[11] A. Mishra, C.-Q. Ma, P. Bäuerle, Chem. Rev. 109 (2009) 1141.
[12] I.F. Perepichka, D.F. Perepichka, Handbook of Thiophene-Based Materials, Wiley-Vch, Weinheim, 2009.
[13] J.-F. Morin, N. Drolet, Y. Tao, M. Leclerc, Chem. Mater. 16 (2004) 4619.
[14] M. Belletête, J. Bouchard, M. Leclerc, G. Durocher, Macromolecules 38 (2005) 880.
[15] J. Lu, P.F. Xia, P.K. Lo, Y. Tao, M.S. Wong, Chem. Mater. 18 (2006) 6194.
[16] V. Promark, A. Pankvuang, S. Ruchirawat, Tetrahedron Lett. 48 (2007) 1151.
[17] V. Promarak, S. Ruchirawat, Tetrahedron 63 (2007) 1602.
[18] V. Promarak, A. Punkvuang, T. Sudyoadsuk, S. Jungsuttiwong, S. Saengsuwan, T. Keawin, K. Sirithip, Tetrahedron 63 (2007) 8881.
[19] M. Belltête, M. Bédard, M. Leclerc, G. Durocher, Synth. Met. 146 (2004) 99.
[20] L. Yang, J.-K. Feng, A.-M. Ren, J.-Z. Sun, Polymer 47 (2006) 1397.
[21] J. Doskocz, M. Doskocz, S. Roszak, J. Soloducho, J.J. Leszczynski, Phys. Chem. A 110 (2006) 13989.
[22] J. Hassan, M. Sevignon, C. Gozzi, E. Schulz, M. Lemaire, Chem. Rev. 102 (2002) 1359.
[23] J. Takagi, K. Takahashi, T. Ishiyama, N. Miyaura, J. Am. Chem. Soc. 124 (2002) 8001.
[24] N. Miyaura, A. Suzuki, Chem. Rev. 95 (1995) 2457.
[25] S.J. Yeh, M.F. Wu, C.T. Chen, Y.H. Song, Y. Chi, M.H. Ho, S.F. Hsu, C.H. Chen, Adv. Mater. 17 (2005) 285.
[26] T.-R. Chen, R.-H. Chien, M.-S. Jan, A. Yeh, J.-D. Chien, J. Organomet. Chem. 691 (2006) 799.
[27] S. Tokito, H. Tanaka, K. Noda, A. Okada, Y. Taga, Appl. Phys. Lett. 70 (1997) 1929.
[28] Z.K. Chen, H. Meng, Y.H. Lai, W. Huang, Macromolecules 32 (1999) 4351.
[29] C. Cai, S.-J. Su, T. Chiba, H. Sasabe, Y.J. Pu, K. Nakayama, J. Kido, Org. Electron. 12 (2011) 843.
[30] C.W. Lee, J.Y. Lee, Adv. Mater. 25 (2013) 5450.